



Rapid Aging as a Key to Understand Deactivation of Ni/Al₂O₃ Catalysts Applied for the CO₂ Methanation

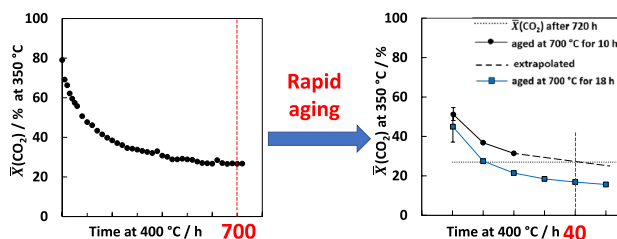
Dennis Beierlein¹ · Dorothea Häussermann¹ · Yvonne Traa¹ · Elias Klemm¹

Received: 17 August 2021 / Accepted: 30 November 2021 / Published online: 15 December 2021
© The Author(s) 2021

Abstract

We developed a rapid aging method for Ni/Al₂O₃ methanation catalysts mimicking the real aging in the actual application. The method is based on hydrothermal deactivation of the catalyst at 600 or 700 °C, which leads to a catalyst with nearly constant conversion after a much shorter time period compared to normal aging. The hydrothermally aged catalysts are characterized by N₂ adsorption, X-ray powder diffraction, temperature-programmed reduction and H₂ chemisorption. The catalytic performance of the aged catalysts is comparable to the one of a catalyst deactivated in a long-term measurement with up to 720 h on stream. The time needed for reaching a stable conversion can be diminished by rapid aging by a factor of 10. The investigations also showed that the long-term deactivation is caused by Ni particle sintering and that the support pores limit the Ni particle size.

Graphical Abstract



Keywords Rapid aging · CO₂ methanation · Ni/Al₂O₃ · Hydrothermal deactivation · Ni particle sintering

1 Introduction

Within the last 20 years, the interest in CO₂ methanation has increased tremendously. The main reason for this increased interest is that the CO₂ methanation can be used for surplus electrical energy storage via the “Power to Gas” (PtG) process [1–4]. The heterogeneously catalyzed CO₂ methanation was first described in 1902 by Sabatier und Senderens [5], and many reviews on CO₂ methanation catalysts have been published since then [6–13]. For an industrial application, a catalyst in the PtG process has to meet certain requirements.

For instance, deactivation is an important phenomenon, which has to be considered for the evaluation of industrial catalysts. The reactor design has to be in line with the time constant of the catalyst deactivation. With respect to laboratory catalyst investigations, deactivation complicates kinetic measurements and scale-up. Especially for catalysts with very long lifetimes as in the automotive sector, the investigation of the reasons for the catalyst deactivation with actual on-road experiments is time-consuming and expensive. Therefore, it is helpful to develop a method for rapid aging of the catalyst in the laboratory, which mimics the real aging in the actual application or in engine benches in a shorter time frame. For realistic conditions, besides adjusting the aging time and temperature, catalyst poisons in the feed, e.g., sulfur compounds, should also be considered [14]. Rapid aging procedures have, to the best of our knowledge, so far

✉ Yvonne Traa
yvonne.traa@itc.uni-stuttgart.de

¹ Institute of Technical Chemistry, University of Stuttgart,
70550 Stuttgart, Germany

mainly been described for automotive emission catalysts, i.e., for the three-way catalyst [15, 16], for diesel oxidation catalysts [14, 16], for lean NO_x trap catalysts [17] or for methane combustion catalysts in lean-operating natural gas engines [16, 18] and for PEM fuel cells [19]. For other applications, there are only a few reports on rapid aging, e.g., for Cu catalysts for methanol synthesis, where sintering is responsible for deactivation [20].

For developing an appropriate rapid aging method, it is important to know the reasons of the catalyst deactivation, which are in most cases coking, poisoning or sintering [21–23]. There are different investigations that deal with the deactivation of Ni catalysts under CO₂ methanation conditions [24–27]. In our previous work on highly loaded Ni/Al₂O₃ catalysts for the CO₂ methanation [24], we also investigated the deactivation of the different catalysts. Since carbonaceous deposits are not thermodynamically favored in the CO₂ methanation [28] and occur to a lesser extent [29, 30], we assumed that the decrease of the Ni surface area due to sintering is the most likely cause for the deactivation. During sintering of metal particles, usually a constant Ni particle diameter or a constant metal surface is reached after an initial phase [24, 31–35]. Thus, the question is after which time period the catalysts reach a constant Ni surface and thereby a constant conversion. Koschany et al. [36] observed on a co-precipitated catalyst ($n_{\text{Ni}}/n_{\text{Al}} = 1$) only after 320 h at 380 °C a constant conversion, and Abelló et al. [37] on another co-precipitated catalyst ($n_{\text{Ni}}/n_{\text{Al}} = 5$) only after 400 h at 400 °C. Dew et al. [38] obtained after aging for 2000 h under different reaction conditions on a commercial Ni/kieselguhr catalyst a constant conversion. In order to avoid this time-consuming and expensive aging, we developed in this work a method for rapid aging of Ni/Al₂O₃ catalysts applied for CO₂ methanation. Our investigations are based on the assumption that the sintering of the Ni particles and of the support is the main cause of deactivation on the long time scale and that carbonaceous deposits are assumed to occur to a lesser extent. Thus, a homogeneous and rapid aging procedure is possible under aggravated hydrothermal conditions.

2 Experimental Section

2.1 Catalyst Preparation

In the present work, a supported catalyst (20 wt% Ni on γ -Al₂O₃) was synthesized via the deposition precipitation technique and labeled with 20DP. The Ni mass fraction is referred to the dry mass of the catalyst in the reduced and passivated state. The catalyst preparation details are described in Beierlein et al. [24]. According to this reference, a suspension of 540 mL of demineralized water and 20 g of γ -Al₂O₃ (Saint-Gobain, 99.90%) was prepared. Next,

27.3 g of Ni(NO₃)₂·6H₂O (Alfa Aesar, 98.3%) was dissolved in 78.6 mL of 1 M HNO₃. This solution was added to the suspension (final pH ≤ 1). Then, a solution of 5 M NaOH (pH ≥ 14) was dosed to the suspension. A flow rate of 500 $\mu\text{L min}^{-1}$ was adjusted via a micrometering pump, and the addition of the alkaline solution was stopped when a pH value of 10 was obtained. After an aging period of 19 h, the suspension was filtered. The filter cake was washed with 200 mL of demineralized water, dried at 150 °C for 12 h and calcined at 400 °C for 3 h. The calcined material was pressed and sieved to a fraction of particles with sizes between 0.200 and 0.315 mm. Finally, a reduction step in a quartz glass reactor at 600 °C for 1 h in 30 vol% hydrogen in nitrogen was conducted and followed by a passivation step in synthetic air. Before the passivation, the catalyst was cooled down to < 30 °C, and the reactor was flushed with nitrogen. Then, oxygen was added, whereby the oxygen content was raised from 0.1 to 1 vol%. Details of the reduction and passivation method can be found in [24, 39].

2.2 Catalyst Characterization

The elemental composition of the reduced and passivated catalyst was investigated via optical emission spectroscopy with inductively coupled plasma (Varian; Vista-MPX CCD 17). The specific surface area, pore volume and pore size distribution were determined by N₂ physisorption. Powder X-ray diffraction analysis was performed with CuK α radiation (30 mA, 40 kV, Bruker AXS, D8 Advance). The mean crystallite size \bar{d}_c was determined from the full width at half maximum of the Ni(200) reflections and corrected using the Warren equation (reference: LaB₆). A Quantachrome Autosorb-iQ apparatus was employed to measure temperature-programmed reduction (TPR). The static H₂ chemisorption method with Quantachrome AUTOSORB-1C was used for the determination of the mean particle size \bar{d}_p , the dispersion D and the Ni surface area $S(\text{Ni})$. Details on TPR and chemisorption measurements and the other methods are reported in [24].

2.3 Experimental Setup

For the rapid aging experiments, 0.5 mm quartz wool and 0.7 g of the reduced and passivated catalyst were placed on the quartz glass frit of a quartz glass reactor. The catalyst was covered with more quartz glass wool, and a thermocouple was placed directly in the middle of the catalyst bed. Great care was taken that the catalyst bed was placed in the isothermal zone of the used tube furnace. The isothermal zone was determined by measuring the temperature gradient of the furnace with a movable thermocouple. The catalyst was heated in 300 mL min⁻¹ H₂ to 600 °C or 700 °C (5 °C min⁻¹). When the temperature was constant, doubly

distilled water was added with a syringe pump (Harvard Instruments), and the water vapor percentage was adjusted to 15 vol% in H₂ (absolute pressure $p_{\text{abs}} = 100$ kPa, $\tau_{\text{mod}} = \text{catalyst mass/total volumetric flow (STP)} = 120$ kg s m⁻³, $\dot{V}_{\text{total}} = 350$ mL min⁻¹). After cooling, the catalyst was passivated (see above).

The catalytic investigation was performed with an automated lab-scale test unit. A detailed description of the test unit can be found in Beierlein et al. [24, 39]. A stainless-steel tube reactor with a diameter of 5 mm was used. The reactor was isothermally heated by an aluminum block, and the temperature was measured with a thermocouple in the first quarter of the fixed bed. For each experiment, 75 mg passivated catalyst was mixed with SiC particles of the same size. A catalyst-SiC dilution ratio of 1/20 was chosen for avoiding hotspots. The blind conversion of SiC was checked at 400 °C and 1.6 MPa. It was proven that the conversion on reactor steel and pure SiC can be neglected (conversions smaller than 1%).

At the beginning of the catalytic tests, the passivated catalysts were re-reduced in 30 vol% H₂/N₂ for 1 h at 400 °C and 0.1 MPa. After reduction, the catalyst was cooled down to room temperature, and a gas mixture of H₂:CO₂:Ar (molar ratio of 76:19:5) was adjusted (modified residence time τ_{mod} of 25 kg s m⁻³). The experiments were conducted at temperatures of 350 and 400 °C at a pressure p of 1.6 MPa. Next, a bypass measurement for determining the accurate gas composition was performed. For the gas analytics, an NDIR detector (URAS26, ABB 3020) and a gas chromatograph (GC, HP 6890) were used. The NDIR detector has the advantage that the concentrations of CO₂, CO and CH₄ can be measured continuously. However, for checking the formation of hydrocarbon byproducts the gas chromatograph was used. Besides CO, only traces of ethane were recognized. The equations for calculating the conversions on the basis of NDIR and GC analytics are described in [24, 39].

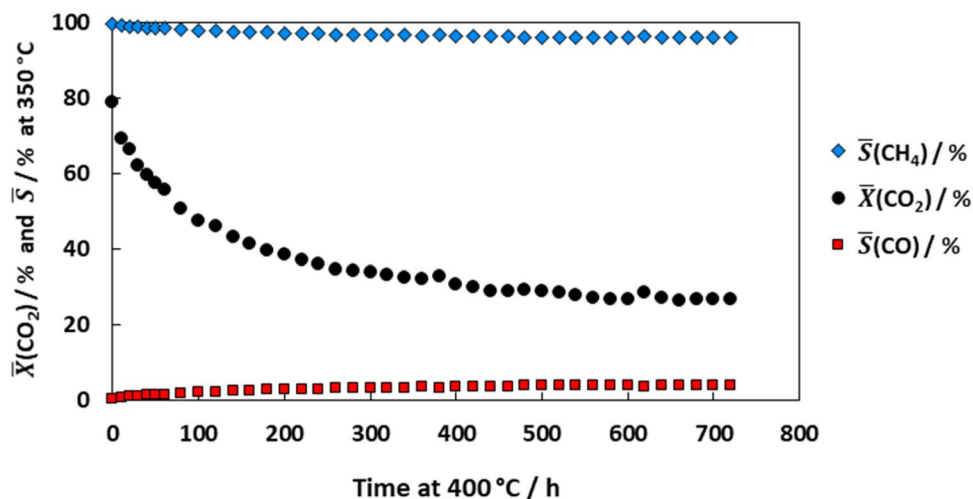
3 Results and Discussion

3.1 Long-Term Stability of the Catalyst

For this work, we chose a catalyst prepared by deposition precipitation with a relatively stable time-on-stream behavior (the most stable catalyst 20DP of our previous work [24]), since the long-term behavior of coprecipitated catalysts has already been investigated by Abelló et al. [37] and Koschany et al. [36]. Generally, the highest reaction temperature and pressure in the power-to-gas process are 400 °C and 1.6 MPa [40], which is why we chose these demanding reaction conditions for our long-term measurement. At 400 °C and 1.6 MPa, even at very low modified residence times ($\tau_{\text{mod}} = 25$ kg s m⁻³), the equilibrium conversion is reached already at the beginning of the experiment. At the equilibrium conversion, the deactivation is concealed by the thermodynamic limitation, and the deactivation cannot be tracked. For an investigation of the deactivation, intermediate reference measurements are performed for 6 h at 350 °C, where the conversion is below the equilibrium conversion. Figure 1 shows the mean conversions $\bar{X}(\text{CO}_2)$ and mean selectivities \bar{S} of the reference measurements at 350 °C over 6 h in dependence of the reaction time of the catalyst at the actual reaction temperature of 400 °C, which leads to the deactivation of the catalyst. Obviously, the catalyst deactivates considerably, especially at the beginning of the measurement. $\bar{X}(\text{CO}_2)$ decreases within the first 10 h at 400 °C from 79 to 69%. After 550 h at 400 °C, a constant conversion of 27% is reached. With decreasing $\bar{X}(\text{CO}_2)$, a slight increase of $\bar{S}(\text{CO})$ can be observed.

Deactivation during catalytic measurements can lead to difficulties and wrong conclusions. If deactivation is not recognized during kinetic measurements, the kinetic

Fig. 1 Mean conversions $\bar{X}(\text{CO}_2)$ and mean selectivities \bar{S} of the reference measurements at 350 °C over 6 h in dependence of the reaction time of the catalyst Ni/ γ -Al₂O₃ at the actual reaction temperature of 400 °C (reaction conditions: molar ratio of H₂:CO₂:Ar = 76:19:5, $\tau_{\text{mod}} = 25$ kg s m⁻³, $p = 1.6$ MPa)



parameters are inaccurate, since they are not only affected by the reaction conditions, but also by the deactivation. However, in kinetic investigations of the CO₂ methanation, deactivation is rarely considered. Koschany et al. [36] explain this with the fact that kinetics are mainly analyzed in the differential regime of the reactor and that deactivation is, under these conditions, usually slow. In order to avoid an influence of the deactivation, meaningful kinetic investigations employ a previously aged catalyst [36, 38]. The aging leads to a constant conversion, so that the influence of the reaction conditions can be observed without errors caused by deactivation. Up to now, it has not been considered, though, that also the aging leads to difficulties because the determined kinetics are only valid for the performance of the specifically aged catalyst. If a fresh catalyst is loaded into an industrial reactor, the significantly higher initial activity of the catalyst can lead to problems with the reactor design (reactor material, cooling system...) and the reliability of its operation. Another serious problem is that the pseudo steady state with constant conversion depends on the specific setup used for aging the catalyst. It will be difficult to transfer these conditions to other systems, since there are, even under the same reaction conditions, inhomogeneities of the concentrations and the temperature in the catalyst bed during aging, since the conversion increases from the beginning to the end of the reactor (Fig. 2). In addition, the temperature and concentration profiles depend on the reactor geometry and the dilution of the catalyst. Especially if the aging temperature is higher than the reaction temperature, where the equilibrium conversion is reached, the reactants are mainly converted in the front part of the reactor. We previously showed that there is a significant temperature gradient in the front part of the reactor, even at dilution of the catalyst with high $m_{\text{SiC}}/m_{\text{catalyst}}$ ratios [39]. Thus, we have to assume that the deactivation depends on the position in the catalyst bed and that the catalyst will be inhomogeneously deactivated over the catalyst bed. Therefore, the transfer of the kinetics of an inhomogeneously aged catalyst between different laboratory reactors, pilot plant and industrial reactors can lead to significant errors, since it

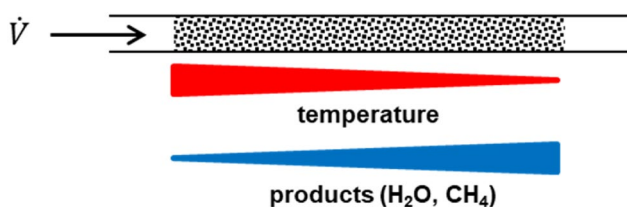


Fig. 2 Scheme of the temperature and concentration gradients during aging under typical reaction conditions of the CO₂ methanation in a fixed-bed reactor

is improbable that the catalyst can be aged to an identical stage.

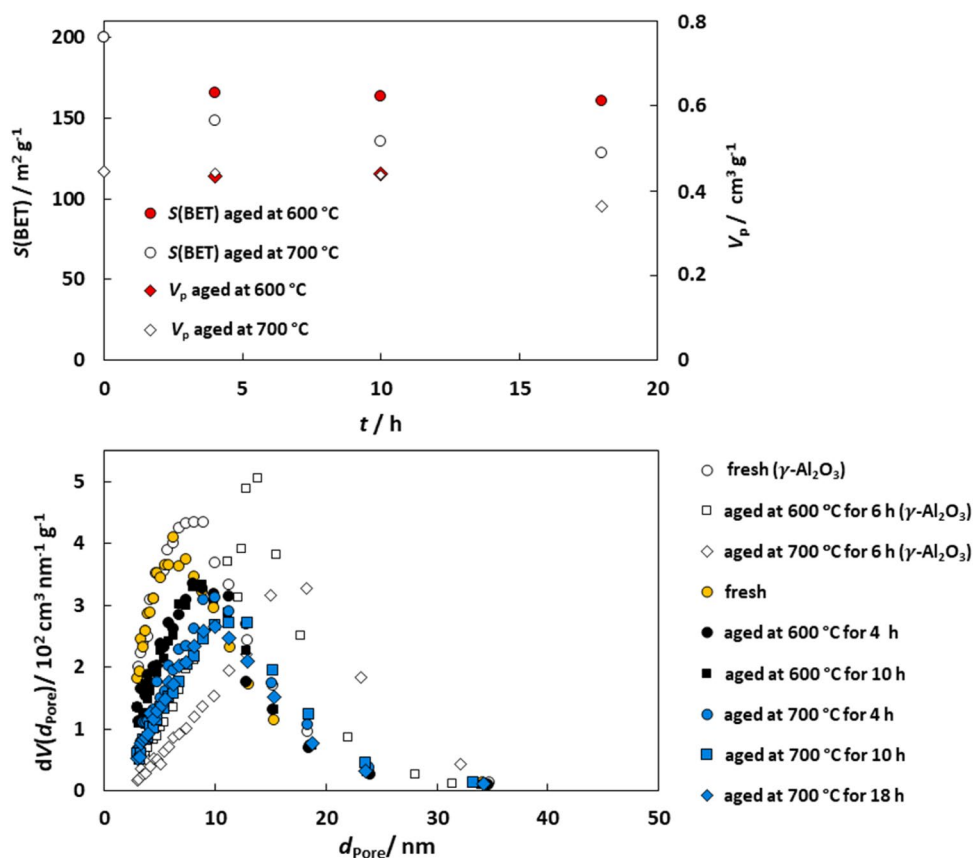
The problems discussed above can be avoided if the catalyst is not aged by normal deactivation during the reaction, but in a homogeneous aging procedure before its use in the actual reaction. Therefore, the aim of this study is to develop a rapid aging method with which the catalyst can be aged fast and homogeneously. Since sintering of the Ni particles is presumably the main reason for the deactivation of the catalyst, a method should be found to accelerate the sintering. It is known that a high temperature and the presence of steam favor the sintering of Ni particles [21, 31, 32, 41]. Even 3 vol% steam (3 kPa H₂O) substantially accelerates sintering of Ni particles [31, 34]. However, at high temperature the H₂O to H₂ ratio should be not too high since this can result in the oxidation of Ni particles to NiO which retards sintering (due to the higher Tamman temperature of NiO). We decided to age the catalyst at 600 °C and 700 °C in H₂ with 15 vol% steam at 100 kPa (15 kPa H₂O). The characterization of the catalysts aged in this manner are discussed in the next chapter.

3.2 Characterization of the Aged Catalyst Samples

First of all, the influence of the aging on the catalyst texture was investigated by N₂ physisorption. Figure 3 shows that the aging leads to a decrease of the BET surface $S(\text{BET})$. The decrease of the BET surface is higher at an aging temperature of 700 °C than at 600 °C. The time dependence of the decrease of $S(\text{BET})$ is at both aging temperatures similar: In the first 4 h, $S(\text{BET})$ decreases considerably. Afterwards, the BET surface does not decrease any more at 600 °C and only slightly at 700 °C. The pore volume stays nearly constant for all aged samples (Fig. 3, top). The pore size distributions of the aged catalysts and pure support samples were determined and compared to the fresh samples (Fig. 3, bottom). A shift of the pore size distribution to larger pore diameters with increasing aging temperature can be observed for the catalyst samples as well as for the support samples. It appears, that the pore size distributions of the pure support samples are located at larger diameters. We assume that this is a consequence of the high Ni loading (Ni mass fraction of 20%): the Ni particles, which are located inside the pores, obviously lead to a pore narrowing effect. In addition, it can be speculated, that the Ni particles stabilize the pore structure of the support. At the same aging temperature, the pore size distributions are very similar. Aging for more than 4 h has no further influence on the texture.

For comparison with the deactivation in methanation feed gas, it would be useful to characterize the spent catalysts after the long-term operation depicted in Fig. 1. Unfortunately, this is not possible. The reasons which do not allow to measure chemisorption after the catalytic experiment are:

Fig. 3 BET surfaces $S(\text{BET})$, pore volumes (V_p) related to the dry total mass of the samples (top) and pore size distributions determined from the adsorption branch (bottom) of the fresh catalyst $\text{Ni}/\gamma\text{-Al}_2\text{O}_3$ and the catalysts aged at different temperatures and aging times t and the aged support $\gamma\text{-Al}_2\text{O}_3$ (aging conditions: 15 vol% steam in H_2 , $p_{\text{abs}} = 100$ kPa, $\tau_{\text{mod}} = 120$ kg s m^{-3} , $\dot{V}_{\text{total}} = 350$ mL min^{-1})



(1) for assuring an isothermal fixed bed, the catalyst has to be diluted with large amounts of SiC. Afterwards, the catalyst cannot be separated from SiC. A separation would only be possible if SiC particles larger than the catalyst particles were used, which is not reasonable since this would lead to bypass streams and channeling. (2) Due to the exothermicity of the reaction, we use only < 75 mg of catalyst. For meaningful characterization with different methods, a higher catalyst mass is needed.

High temperatures and steam can lead to a change of the modification of the $\gamma\text{-Al}_2\text{O}_3$ support [42, 43]. However, a comparison of the X-ray powder diffraction patterns in Fig. 4 of the pure support before aging and the different aged samples does not give any indication that the support changes during the thermal treatment. The Al_2O_3 reflections are shifted to higher diffraction angles than the value of the reference data base (JCPDS 00-010-0425). This is in accordance with the XRD pattern of the pure Al_2O_3 support. Thus, it can be assumed that this is caused by the Al_2O_3 modification of the specific support used in this work.

Only Ni reflections and no NiO reflections can be seen. The Ni reflections of the aged samples are significantly narrower than the Ni reflections of the fresh sample. After aging at 700 °C, the Ni reflections are slightly narrower than after aging at 600 °C. Therefore, a higher aging

temperature leads to larger Ni crystallites, whereas the aging time (longer than 4 h) has no influence on the crystallite size.

XRD analysis is a powerful tool for identifying the crystalline bulk phase composition of a catalyst. However, the formation of amorphous phases or surface compounds are not visible in the XRD patterns. A well-known method to investigate oxidic Ni surface compounds, like Ni surface aluminates, is the temperature-programmed reduction (TPR) technique. The reducibility of Ni^{2+} ions in solid-state reactions depends on the specific coordination environment. Thus, the TPR method is a surface-sensitive method suitable for identifying different Ni species according to their different reduction temperatures. With the adjusted TPR conditions, pure nickel oxide (NiO) is reduced between 200 and 400 °C [24]. The Ni species with an interaction between the Ni^{2+} ions and the Al_2O_3 support (likely non-stoichiometric and stoichiometric Ni aluminates NiAl_2O_4) show higher reduction temperatures [24]. With our samples, even after the longest aging time of 18 h at the highest aging temperature of 700 °C, no difficulties to reduce Ni species can be observed (Fig. 5). A comparison with the calcined sample shows that the aged samples bear only easily reducible NiO (passivation layer). Thus, the formation of surface Ni aluminates in the aged samples can be excluded.

Fig. 4 X-ray powder diffraction patterns of the fresh and the aged catalysts Ni/ γ -Al₂O₃ in the passivated state compared to the calcined γ -Al₂O₃ support. Ni (JCPDS 00-001-1258) and γ -Al₂O₃ (JCPDS 00-010-0425) are indicated with vertical lines (aging conditions: 15 vol% steam in H₂, p_{abs} = 100 kPa, τ_{mod} = 120 kg s m⁻³, \dot{V}_{total} = 350 mL min⁻¹)

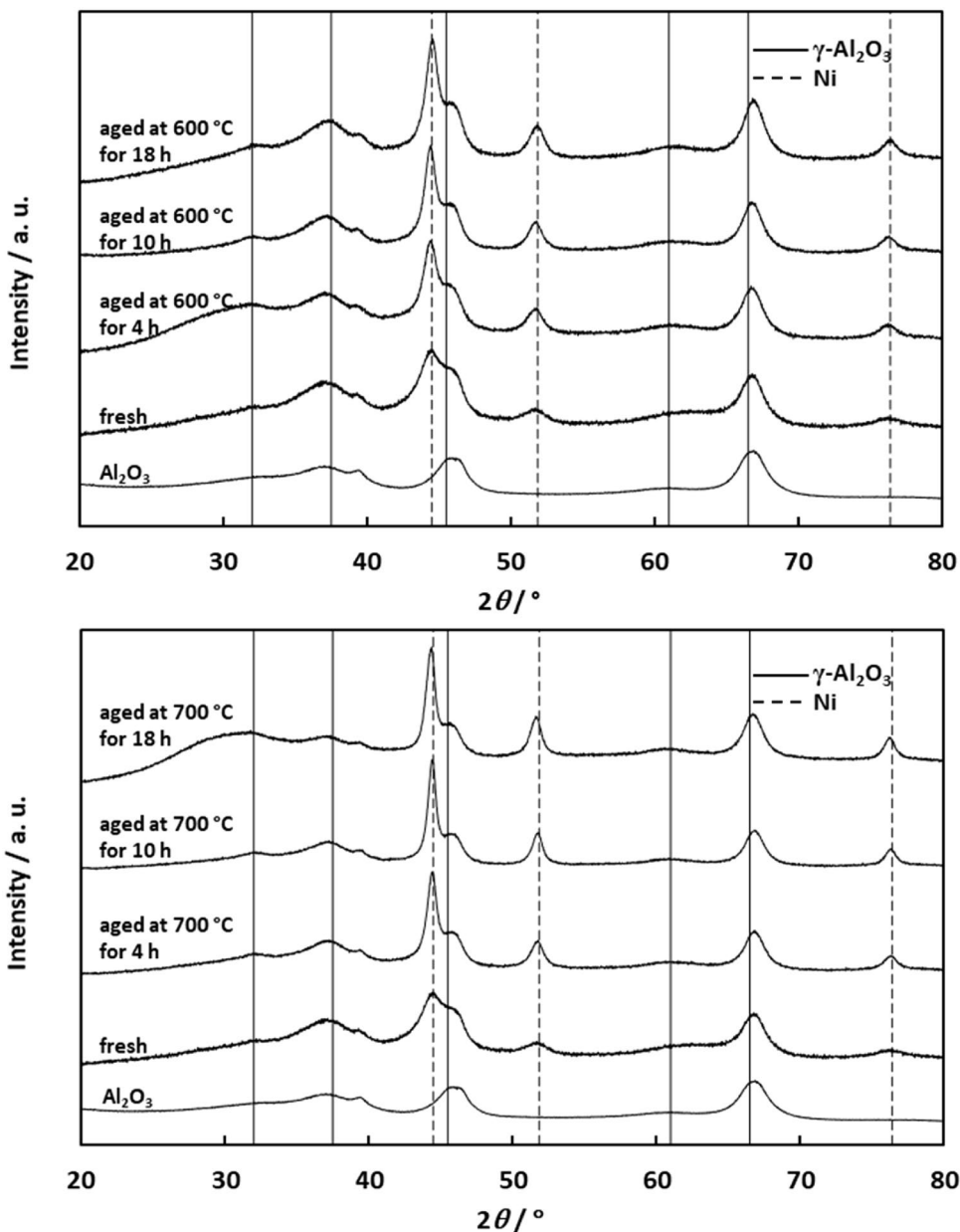


Fig. 5 Temperature-programmed reduction profile of the calcined catalyst Ni/ γ -Al₂O₃ and the reduced and passivated catalyst before and after aging (aging conditions: 15 vol% steam in H₂, p_{abs} = 100 kPa, τ_{mod} = 120 kg s m⁻³, \dot{V}_{total} = 350 mL min⁻¹)

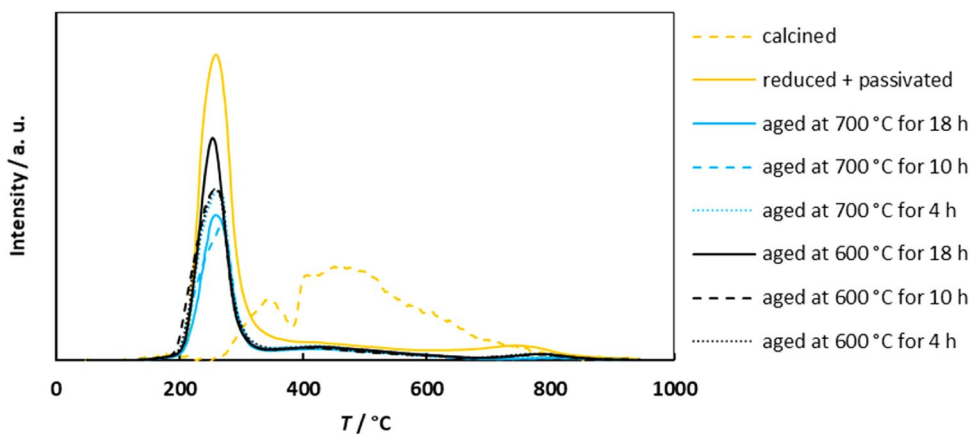
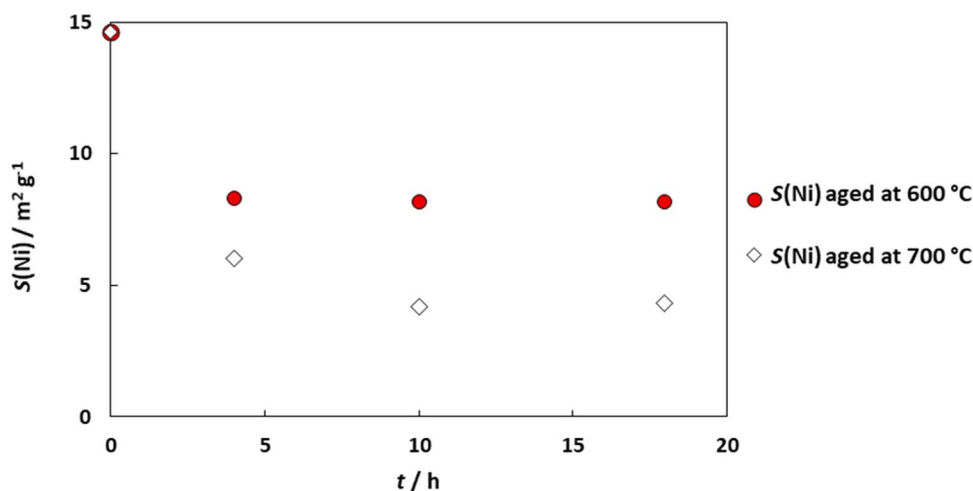


Fig. 6 Metal surfaces $S(\text{Ni})$ of the aged catalysts $\text{Ni}/\gamma\text{-Al}_2\text{O}_3$ in dependence of the aging time t as determined by H_2 chemisorption (aging conditions: 15 vol% steam in H_2 , $p_{\text{abs}} = 100$ kPa, $\tau_{\text{mod}} = 120$ kg s m^{-3} , $\dot{V}_{\text{total}} = 350$ mL min^{-1})



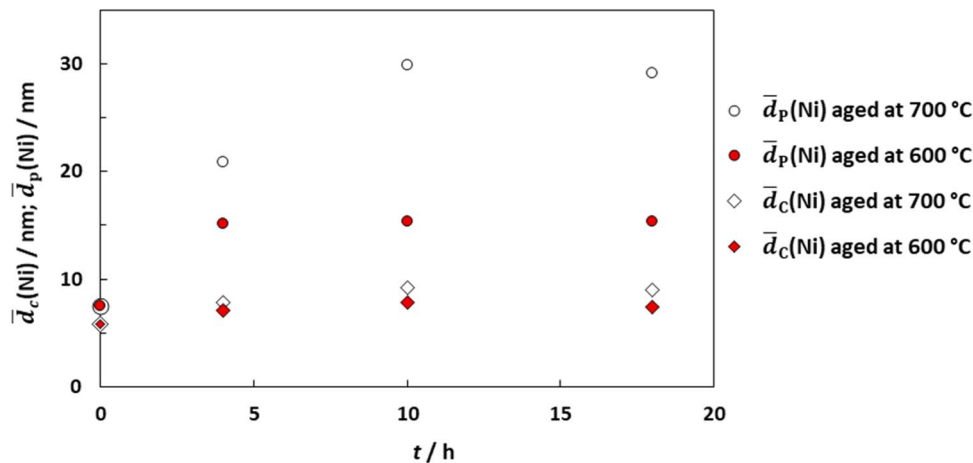
The Ni surface area is determined with H_2 chemisorption. Figure 6 shows that the metal surface decreases strongly within the first 4 h of the aging. Stabilization of the surface is achieved after 4 h (600 °C) and after 10 h (700 °C). After aging at 700 °C, the metal surface decreases more strongly than after aging at 600 °C. It is also noticeable that the decrease of the metal surface is more significant than the decrease of the BET surface.

Bartholomew et al. [22] explain the decrease of the metal and the BET surface of a $\text{Ni}/\text{Al}_2\text{O}_3$ catalyst in a steam-containing atmosphere with a blocking of the pores caused by sintering metal particles. Due to the blocking of the pores, a part of the metal particles and of the BET surface is not accessible any more. The assumption is based on the observation that the pore volume decreases whereas the pore diameter stays constant. In contrast to Bartholomew et al. [22], the pore volume in this work stays constant, whereas the pore diameter increases (Fig. 3). A constant pore volume with decreasing BET surface and increasing pore diameter is characteristic of the sintering of $\gamma\text{-Al}_2\text{O}_3$ [24]. Our previous

work also showed that the Ni particles are stabilized as soon as the size of the metal particles reaches the pore diameter [24]. The pore size distributions in Fig. 3 show that the pore diameters increase during aging. Therefore, the metal particles should become mobile and sinter until the particle size and the pore diameter match again. And actually, after aging at 600 °C, the mean pore diameter of the $\gamma\text{-Al}_2\text{O}_3$ support agrees with the mean Ni particle size of the stable state (Fig. 3: $\bar{d}_{\text{pore}}(\gamma\text{-Al}_2\text{O}_3) = 14$ nm, Fig. 7: $\bar{d}_p(\text{Ni}) = 15$ nm).

After aging at 700 °C, the particle diameter of the stable state is somewhat larger than the mean pore diameter. This can be explained with the fact that the support is only aged for 6 h at 700 °C. Figure 3 shows that the BET surface decreases during aging at 700 °C also further between 4 and 10 h. Thus, the pore diameter of the support could be larger after aging for 10 h. And indeed, the mean Ni particle size after aging for 4 h agrees quite well with the mean pore diameter of the support after aging for 6 h (Fig. 3: $\bar{d}_{\text{pore}}(\gamma\text{-Al}_2\text{O}_3) = 18$ nm, Fig. 7: $\bar{d}_p(\text{Ni}) = 21$ nm). With the stabilizing effect of the support, the coupling between the metal and the

Fig. 7 Mean particle sizes $\bar{d}_p(\text{Ni})$ determined by H_2 chemisorption and mean crystallite sizes $\bar{d}_c(\text{Ni})$ of the catalysts $\text{Ni}/\gamma\text{-Al}_2\text{O}_3$ determined by XRD (aging conditions: 15 vol% steam in H_2 , $p_{\text{abs}} = 100$ kPa, $\tau_{\text{mod}} = 120$ kg s m^{-3} , $\dot{V}_{\text{total}} = 350$ mL min^{-1})



BET surface can be understood: During the initial decrease of the BET surface, a significant decrease of the metal surface can be observed. When the BET surface and the support texture (pore diameter) are stabilized (more than 4 h aging at 600 °C; more than 10 h aging at 700 °C), the metal surface stays constant. The mean Ni crystallite sizes are significantly smaller than the mean Ni particle sizes and increase only little with increasing aging time. The difference is presumably due to the fact that the Ni crystallites agglomerate to larger particles consisting of several crystallites [41].

TEM measurements could additionally prove this assumption. However, it is known that the contrast between the γ -Al₂O₃ support and the Ni particles is very weak and that Ni particles cannot be clearly distinguished from the support [41, 44–46]. Thus, particle size measurements of Ni particles on γ -Al₂O₃ can reliably only be conducted with special techniques like microdiffraction [46] or HAADF [41]. With common TEM measurements, the question whether the Ni particles are located inside the pores of γ -Al₂O₃ can usually not be answered.

The discussion shows that the stabilizing effect of the mesopores can explain why the metal surface reaches a pseudo-steady-state value when the texture of the support is stabilized and the particle diameter agrees with the pore diameter of the support. Other suggested explanations such as the attachment to convex regions [21, 47] are less plausible and do not explain the difference between the catalysts after aging at 600 °C and 700 °C satisfactorily. With different pore diameters, the difference between the steady states of different aging temperatures can be clearly clarified: The pseudo steady state of the particle size is different because the pore diameter varies with the aging temperature.

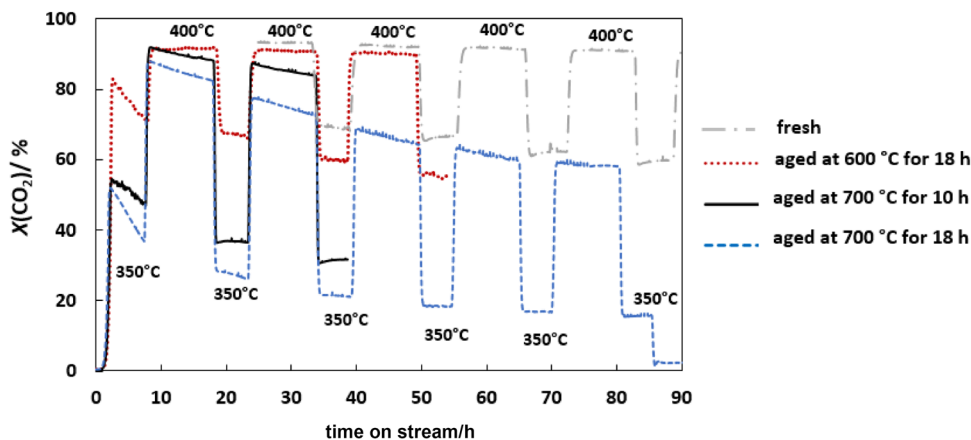
Ruckenstein and Pulvermacher [48] investigated as early as 1975 the influence of the support texture on the sintering of metal particles. They hypothesize that the pore diameter limits the particle size during sintering of metal particles. This hypothesis was rejected in known publications on the

sintering of Ni on various supports [32, 41, 49]. In these publications, the BET surface and the support only have a small influence on the sintering of metal particles. In addition, the more recently published kinetic laws for the description of the sintering of Ni particles hint at a small effect of the support [49]. In a newer review on CO₂ methanation, some of this older work is cited as a basis for the understanding of the catalyst deactivation [50]. However, it is ignored that these publications investigate the sintering of Ni on supports with a small BET surface of 20 to 50 m² g⁻¹ and no pronounced porosity [32, 41, 49]. During the derivation of the kinetic laws, the pore structure is not involved so that the stabilizing effect of the texture is not considered. However, the results and the discussion in this work demonstrate a significant influence of the support texture which supports the pioneering work of Ruckenstein and Pulvermacher [48] which should be given more attention.

3.3 Catalytic Performance of the Aged Catalyst Samples

The time-on-stream behavior of the catalysts aged at 600 to 700 °C for 10 to 18 h in H₂ with 15 vol% steam is shown in Fig. 8. First, the conversion is determined at 350 °C for 6 h. Afterwards, it is alternately measured at 400 °C for 10 h and at 350 °C for 6 h. On the catalyst aged at 600 °C for 18 h, an initial conversion of 83% is observed at 350 °C, which decreases significantly with increasing time on stream. The catalysts aged at 700 °C reach a significantly lower initial conversion. Our previous work [24] showed that the conversion correlates linearly with the metal surface. Therefore, we can assume that the difference in the initial conversion is proportional to the metal surface of the catalysts. Actually, the relative difference between the conversions of the catalyst aged at 700 °C for 18 h and the one aged at 600 °C for 18 h agree pretty well with the relative difference of the metal surfaces ($\Delta X(\text{CO}_2)_{t=0} = 39$ rel.%; $\Delta S(\text{Ni})_{t=0} = 47$ rel.%). The small conversion difference between the catalysts

Fig. 8 Time-on-stream behavior of the fresh and chosen aged Ni/ γ -Al₂O₃ catalysts at $T = 350$ °C (small conversions) and 400 °C (higher conversions) (reaction conditions: molar ratio of H₂:CO₂:Ar = 76:19:5, $\tau_{\text{mod}} = 25$ kg s m⁻³, $p = 1.6$ MPa; aging conditions: 15 vol% steam in H₂, $p_{\text{abs}} = 100$ kPa, $\tau_{\text{mod}} = 120$ kg s m⁻³, $\dot{V}_{\text{total}} = 350$ mL min⁻¹)



aged at 700 °C for 10 h and the ones aged at 700 °C for 18 h can be explained with the similar metal surfaces ($S(\text{Ni})=4.2 \text{ m}^2 \text{ g}^{-1}$ (10 h), $S(\text{Ni})=4.3 \text{ m}^2 \text{ g}^{-1}$ (18 h)) of these catalysts.

The measurement of the fresh catalyst did not start with a measurement at 350 °C, but with a slow temperature ramp (not shown here), whereupon the conversion at 400 °C is measured. Afterwards, the temperature is lowered to 350 °C. The fresh sample reaches a higher conversion at 350 °C compared with the aged samples. This indicates the smaller extent of deactivation for the fresh sample. This sample reaches the equilibrium conversion in the following measurements at 400 °C, and hence, no deactivation can be observed.

It is noticeable that the catalysts undergo a different decrease of the conversion, which follows, at a reaction temperature of 350 °C, the trend between 2 and 8 h on stream: aged at 700 °C for 18 h (-3.0% per h) > aged at 600 °C for 18 h (-2.3% per h) > aged at 700 °C for 10 h (-1.4% per h). The strong deactivation during the first 8 h on stream at 350 °C when conducting the CO_2 methanation is unexpected, and it is very unlikely that Ni sintering is the reason because—as discussed in the section on characterization—the Ni sintering during rapid aging already reached a maximum particle size dictated by the pore size. Sintering is very temperature-sensitive [32] which suggests that a distinct deactivation at 350 °C after 18 h at 700 °C may not be caused by sintering although the H_2O partial pressure is higher. Thus, we speculate that it is much more likely that (1) the Ni surface is restructured or (2) blocked by the accumulation of surface species such as formates or carbonates, (3) formation of hydroxide species occurs ($\text{Ni}(\text{OH})_2/\text{Al}(\text{OH})_3$) or that (4) the support surface is changed by a loss of acidic/basic sites. However, for determining this additional cause of deactivation further surface-sensitive investigations are needed like in situ XPS.

When switching to a reaction temperature of 400 °C, the catalyst aged at 600 °C for 18 h reaches the equilibrium conversion. The catalyst aged at 700 °C for 10 h starts with the

equilibrium conversion, but the conversion decreases with increasing time on stream. On the catalyst aged at 700 °C for 18 h, the conversion reached at 400 °C is, due to the strong deactivation at 350 °C, smaller than on the catalyst aged at 700 °C for 10 h. Both catalysts aged at 700 °C have a similar conversion decrease at a reaction temperature of 400 °C ($\approx -0.5\%$ per h). After the second measurement at 400 °C, no deactivation at 350 °C can be perceived any more, and further deactivation can only be observed during the reaction at 400 °C. This shows that the catalyst deactivates more strongly at 400 °C than at 350 °C. Therefore, the temperature and the partial pressure of steam should have the strongest influence on the deactivation. However, if the equilibrium conversion is reached (as at 400 °C in Fig. 1), a decreasing residence time should also cause a faster deactivation: At the equilibrium conversion, the catalyst is kinetically able to convert more reactants, but is thermodynamically limited. If more reactants are supplied due to a decreasing residence time, then more reactants can be converted at the front part of the fixed bed. This should cause a higher heat release with a higher hot spot temperature [39], leading to a faster deactivation rate. With further decreasing residence time, a point should be reached at which the catalyst is not able any more to convert all reactants up to the extent of the equilibrium conversion. Hence, a lower conversion should result causing a lower partial pressure of the reaction product steam. The higher flow rate of the lower residence time should also decrease the hot spot temperature due to higher convective heat transport. Thus, a lower deactivation rate is expected with a further decreasing residence time.

For a comparison of the conversion of the aged catalysts with the constant conversion of the long-term measurement, the mean conversions at 350 °C are plotted versus the reaction time at 400 °C (Fig. 9). The deactivation during the measurement at 350 °C is given as indication bar. The top of the indication bar states the conversion at the beginning of the 350 °C measurement. During the measurement at constant temperature, the conversion decreases. At the end

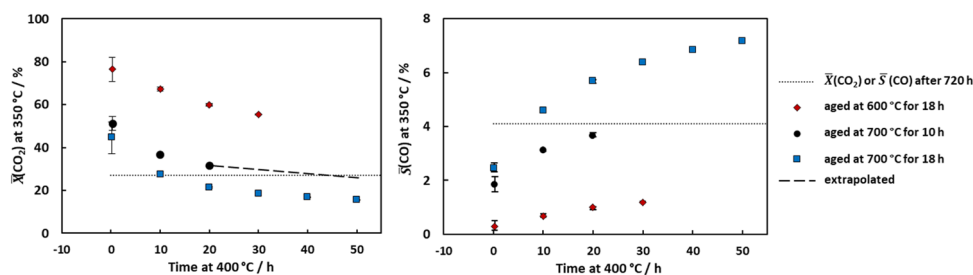
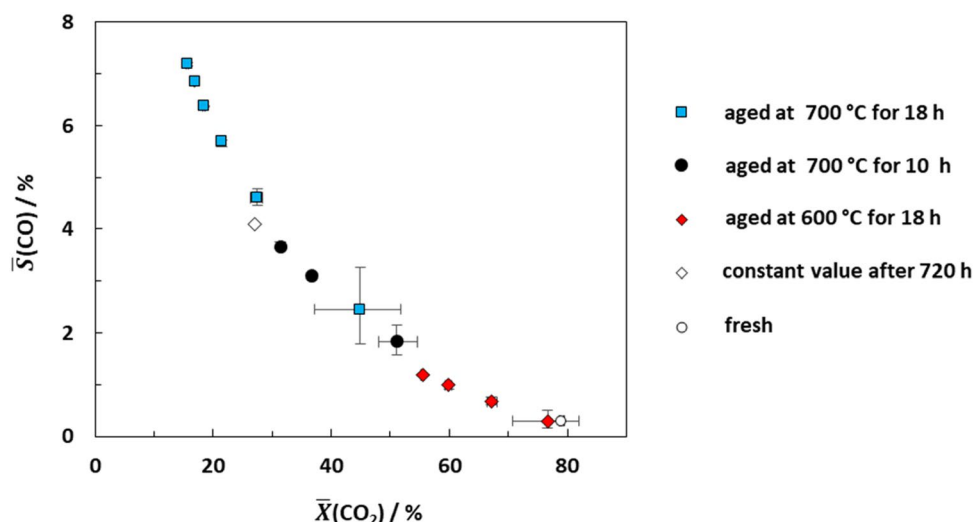


Fig. 9 Mean conversions $\bar{X}(\text{CO}_2)$ (left) and mean selectivities $\bar{S}(\text{CO})$ (right) of chosen aged $\text{Ni}/\gamma\text{-Al}_2\text{O}_3$ catalysts of the reference measurements at 350 °C over 6 h in dependence of the reaction time of the catalyst at 400 °C. The indication bar indicates the decrease of $\bar{X}(\text{CO}_2)$ and the increase of $\bar{S}(\text{CO})$ at 350 °C. The dotted horizontal

lines give the constant conversion and selectivity to CO of the long-term experiment after 720 h in Fig. 1 (reaction conditions: molar ratio of $\text{H}_2:\text{CO}_2:\text{Ar}=76:19:5$, $\tau_{\text{mod}} = 25 \text{ kg s m}^{-3}$, $p=1.6 \text{ MPa}$; aging conditions: 15 vol% steam in H_2 , $p_{\text{abs}} = 100 \text{ kPa}$, $\tau_{\text{mod}} = 120 \text{ kg s m}^{-3}$, $\dot{V}_{\text{total}} = 350 \text{ mL min}^{-1}$)

Fig. 10 Mean CO selectivities $\bar{S}(\text{CO})$ in dependence of the mean conversions $\bar{X}(\text{CO}_2)$ of chosen aged Ni/ γ -Al₂O₃ catalysts of the reference measurements at 350 °C over 6 h. The indication bars indicate the decrease of $\bar{X}(\text{CO}_2)$ and the increase of $\bar{S}(\text{CO})$ at 350 °C (reaction conditions: molar ratio of H₂:CO₂:Ar=76:19:5, $\tau_{\text{mod}} = 25 \text{ kg s m}^{-3}$, $p = 1.6 \text{ MPa}$; aging conditions: 15 vol% steam in H₂, $p_{\text{abs}} = 100 \text{ kPa}$, $\tau_{\text{mod}} = 120 \text{ kg s m}^{-3}$, $\dot{V}_{\text{total}} = 350 \text{ mL min}^{-1}$)



of the measurement, the conversion reaches the lower limit of the indication bar. The mean conversion of the catalyst aged at 600 °C for 18 h is even after 30 h reaction at 400 °C significantly larger than the constant conversion of the long-term measurement plotted as dotted horizontal line. The mean conversion decrease of the catalyst aged at 700 °C for 10 h is within the first 20 h comparable to the catalyst aged at 700 °C for 18 h. Thus, we assume that the catalyst aged at 700 °C for 10 h should also, after a reaction time of 20 to 50 h at 400 °C, show a comparable conversion decrease. After 50 h at 400 °C, the conversion of the catalyst aged at 700 °C for 18 h approaches a constant value which should also be the case for the catalyst aged at 700 °C for 10 h. This value should agree with the value of the long-term measurement. Therefore, we suggest the following rapid aging method: First, the catalyst is hydrothermally aged for 10 h at 700 °C in 15 vol% steam in H₂. Then, the catalyst is further stabilized during methanation at 400 °C and 1.6 MPa for 50 h. As compared to the long-term measurement under the same harsh methanation conditions, where a constant conversion is only reached after 550 h on stream, this means that the time needed for reaching a constant conversion can be diminished by a factor of 10 by implementing the suggested rapid aging method.

Finally, we want to have a look at the selectivity to CO (Fig. 9 right): the CO selectivity increases with increasing time on stream at 400 °C. During the first measurement at 350 °C, the selectivity to CO increases (indication bars in Fig. 9: at the beginning of the 350 °C measurement, the CO selectivity is stated by the lower end of the indication bar. After 6 h at 350 °C, the CO selectivity reaches the higher end of the indication bar). Since the conversion changes and $\bar{S}(\text{CO})$ depends on the conversion ($S(\text{CO}) X(\text{CO}_2)$ coupling), Fig. 9 does not show whether the conversion decrease is the reason for the increase of $\bar{S}(\text{CO})$ or whether the deactivation

has a direct influence on $\bar{S}(\text{CO})$. To separate the influence of the conversion decrease from the influence of the deactivation on $\bar{S}(\text{CO})$, the mean conversions and the mean CO selectivities at 350 °C of the fresh catalyst (first measured point of Fig. 1) are plotted in an S - X diagram and compared to the values of the aged catalyst samples (Fig. 10). The indication bars indicate the decrease of the conversion and the increase of $\bar{S}(\text{CO})$ during the measurement at 350 °C. It can be seen that the initial S - X values at the beginning of the measurements with the aged catalysts agree with the values of the fresh catalyst (right corner at the bottom of the squares which is spanned by the indication bars).

The S - X -values of fresh catalyst, aged catalysts and the limit of the long-term measurement after 720 h (Fig. 1) lie on a trajectory. This indicates that the CO selectivity is not influenced by an aging effect other than conversion decay, neither by the short-term deactivation (conditioning) nor by the long-term deactivation. It is assumed that the change in CO selectivity is only due to the conversion decrease. The CO selectivity is, therefore, not a descriptor for the deactivation.

4 Conclusions and Outlook

The physical characterization of the aged catalyst reveals a distinct increase of the Ni particle size and a decrease of the Ni surface area. It was shown that the support texture has a significant influence on the sintering: The pore diameter of the support varies with the aging temperature, and a constant particle size is only obtained when Ni particles reach the same diameter as the pores.

A short-term deactivation (conditioning) and a long-term deactivation were observed. The short-term deactivation is

presumably a result of restructured or oxidized Ni surface and/or the accumulation of surface species such as formates or carbonates. Long-term deactivation is caused by Ni particle sintering. Since both kinds of deactivation have an important influence on the performance of the catalyst, we suggest the following rapid aging method for Ni/Al₂O₃ methanation catalysts: First, the catalyst is hydrothermally aged for 10 h at 700 °C in 15 vol% steam in H₂. Then, the catalyst is further stabilized during methanation at 400 °C and 1.6 MPa for 50 h. In this way, the aging time to reach a pseudo-steady-state conversion can be diminished by a factor of 10.

However, we can not exclude an inhomogeneous deactivation of the catalyst bed in the second step, since the conversion of CO₂ results in concentration and temperature gradients during the reaction. A possibility for a fully homogeneous deactivation could be the following: First, the above-described rapid aging method is employed to reach a homogeneous deactivation due to sintering. Afterwards, the aged catalysts are further deactivated at small conversions and small residence times (large volumetric flow rates). Due to the small conversions and the high flow rates, the concentration and temperature profiles in the catalyst should be small, similar to the situation in the differential regime of a reactor. If this method is not possible, there are different alternatives: (i) Accepting the uncertainty for the transfer of the kinetics of specifically aged catalysts; (ii) laborious determination of the deactivation kinetics; (iii) empirical investigations in pilot plants under nearly identical conditions of the envisaged commercial plant; (iv) development of a catalyst which does not deactivate under the targeted reaction conditions.

Acknowledgements The authors thank Mirko Pfeifer, Prof. Thomas Schwarz and Prof. Klaus Stöwe for providing the catalyst.

Funding Open Access funding enabled and organized by Projekt DEAL.

Declarations

Conflict of interest The authors declare that there is no conflict of interest.

Open Access This article is licensed under a Creative Commons Attribution 4.0 International License, which permits use, sharing, adaptation, distribution and reproduction in any medium or format, as long as you give appropriate credit to the original author(s) and the source, provide a link to the Creative Commons licence, and indicate if changes were made. The images or other third party material in this article are included in the article's Creative Commons licence, unless indicated otherwise in a credit line to the material. If material is not included in the article's Creative Commons licence and your intended use is not permitted by statutory regulation or exceeds the permitted use, you will need to obtain permission directly from the copyright holder. To view a copy of this licence, visit <http://creativecommons.org/licenses/by/4.0/>.

References

- Götz M, Lefebvre J, Mörs F, Koch AM, Graf F, Bajohr S, Reimert R, Kolb T (2016) *Renew Energy* 85:1371–1390
- Schiebahn S, Grube T, Robinius M, Tietze V, Kumar B, Stolten D (2015) *Int J Hydrogen Energy* 40:4285–4294
- Lewandowska-Bernat A, Desideri U (2018) *Appl Energy* 228:57–67
- Thema M, Bauer F, Sterner M (2019) *Renew Sustain Energy Rev* 112:775–787
- Sabatier P, Senderens JB (1902) *Acad Sci* 134:514–516
- Mills GA, Steffgen FW (1974) *Catal Rev* 8:159–210
- Watson GH (1980) Methanation catalysts. Report number ICTIS/TR 09. International Energy Agency, Coal Research, London
- Krylov OV, Mamedov KH (1995) *Russ Chem Rev* 64:877–900
- Wang W, Gong J (2011) *Front Chem Sci Eng* 5:2–10
- Aziz MAA, Jalil AA, Triwahyono S, Ahmad A (2015) *Green Chem* 17:2647–2663
- Li W, Wang H, Jiang X, Zhu J, Liu Z, Guo X, Song C (2018) *RSC Adv* 8:7651–7669
- Miao B, Ma SSK, Wang X, Su H, Chan SH (2016) *Catal Sci Technol* 6:4048–4058
- Nie X, Li W, Jiang X, Guo X, Song C (2019) *Adv Catal* 65:121–233
- Andersson J, Antonsson M, Eurenus L, Olsson E, Skoglundh M (2007) *Appl Catal B* 72:71–81
- Kallinen K, Supanki A, Härkönen M (2005) *Catal Today* 100:223–228
- Maunula T, Kallinen K, Savimäki A, Wolff T (2016) *Top Catal* 59:1049–1053
- De Abreu GJ, Kristoffersson A, Wentworth T, Olsson L (2018) *Ind Eng Chem Res* 57:9362–9373
- Auvinen P, Kinnunen NK, Hirvi JT, Maunula T, Kallinen K, Keenan M, Baert R, van den Tillaart E, Suvanto M (2019) *Appl Catal B* 258:117976
- Zhang S, Yuan XZ, Ng Cheng Hin J, Wang H, Friedrich KA, Schulze M (2009) *J Power Sources* 194:588–600
- Kurtz M, Wilmer H, Genger T, Hinrichsen O, Muhler M (2003) *Catal Lett* 86:77–80
- Ertl G, Knözinger H, Schüth F, Weitkamp J (eds) (2008) *Handbook of heterogeneous catalysis*, vol 4. Wiley-VCH, Weinheim, pp 1829–1846
- Bartholomew CH, Pannell RB, Fowler RW (1983) *J Catal* 79:34–46
- Forzatti P (1999) *Catal Today* 52:165–181
- Beierlein D, Häussermann D, Pfeifer M, Schwarz T, Stöwe K, Traa Y, Klemm E (2019) *Appl Catal B Environ* 247:200–219
- Ewald S, Kolbeck M, Kratky T, Wolf M, Hinrichsen O (2019) *Appl Catal A* 570:376–386
- Burger T, Koschany F, Thomys O, Köhler K, Hinrichsen O (2018) *Appl Catal A* 558:44–54
- Wolf M, Schüler C, Hinrichsen O (2019) *J CO₂ Util* 32:80–91
- Gao J, Wang Y, Ping Y, Hu D, Xu G, Gu F, Su F (2012) *RSC Adv* 2:2358–2368
- Solymosi F, Erdöhelyi A, Bánsági T (1981) *J Catal* 68:371–382
- Ocampo F, Louis B, Roger AC (2014) *Appl Catal A* 369:90–96
- Delmon B, Froment GF (eds) (1994) *Catalyst deactivation 1994, studies in surface science and catalysis*, vol 88. Elsevier, Amsterdam, pp 1–18
- Sehested J, Gelten JAP, Helveg S (2006) *Appl Catal A* 309:237–246
- Richardson JT, Crump JG (1979) *J Catal* 57:417–425
- Bartholomew CH (1993) *Appl Catal A* 107:1–57

35. Bartholomew CH, Fuentes GA (eds) (1997) Catalyst deactivation 1997, studies in surface science and catalysis, vol 111. Elsevier, Amsterdam, pp 585–592
36. Koschany F, Schlereth D, Hinrichsen O (2016) Appl Catal B 181:504–516
37. Abelló S, Berruoco C, Montané D (2013) Fuel 113:598–609
38. Dew JN, White RR, Sliepcevich CM (1955) Ind Eng Chem 47:140–146
39. Beierlein D, Schirmer S, Traa Y, Klemm E (2018) Reac Kinet Mech Cat 125:157–170
40. Buchholz OS, van der Ham AGJ, Veneman R, Brilman DWF, Kersten SRA (2014) Energy Procedia 63:7993–8009
41. Sehested J, Carlsson A, Janssens TVW, Hansen PL, Datye AK (2001) J Catal 197:200–209
42. Schüth F, Sing KSW, Weitkamp J (eds) (2002) Handbook of porous solids. Wiley, Weinheim, pp 1591–1677
43. Bartholomew CH, Butt JB (eds) (1991) Catalyst deactivation 1991, studies in surface science and catalysis, vol 68. Elsevier, Amsterdam, pp 29–51
44. Mustard DG, Bartholomew CH (1981) J Catal 67:186–206
45. Poncelet G, Centeno MA, Molina R (2005) Appl Catal A 288:232–242
46. Lamber R, Schulz-Ekloff G (1991) Surf Sci 258:107–118
47. Wynblatt P, Gjostein NA (1975) Prog Solid State Chem 9:21–58
48. Ruckenstein R, Pulvermacher B (1975) J Catal 37:416–423
49. Sehested J, Gelten JAP, Remediakis IN, Benggaard H, Nørskov JK (2004) J Catal 233:432–443
50. Gao J, Liu Q, Gu F, Liu B, Zhong Z, Su F (2015) RSC Adv 5:22759–22776

Publisher's Note Springer Nature remains neutral with regard to jurisdictional claims in published maps and institutional affiliations.